

Optical orientation and probe-field spectroscopy of metastable atoms

S. G. Rautian

Institute of Automatic Systems and Electrometry, Siberian Branch of the Russian Academy of Sciences, 630090 Novosibirsk, Russia

A. V. Shishaev

Institute of Semiconductor Physics, Siberian Branch of the Russian Academy of Sciences, 630090 Novosibirsk, Russia

Zh. Éksp. Teor. Fiz. **108**, 807–828 (September 1995)

The problem of the probe-field spectroscopy of optical transitions in atomic systems with a degenerate metastable lower state during optical pumping in a polarized field of arbitrary intensity is studied. It is shown for the particular case when the total angular momenta of the lower and excited states of the transition are equal ($J_n = J_m \geq 2$) that, because the levels are degenerate and are excited anisotropically, the absorption spectrum of the probe field contains, besides resonances caused by occupancy effects, resonances associated with the magnetic coherence and manifested in the form of peaks and dips with substantially different amplitudes and widths. A fundamentally new property of these resonances is that their widths are proportional to the intensity of the orienting field, and the amplitude of the narrowest resonance becomes appreciable when the orienting field is very strong. © 1995 American Institute of Physics.

1. INTRODUCTION

The optical orientation of atoms which arises when the atoms interact with nonequilibrium radiation—polarized, directed, and spectrally selective—is being intensively studied (see, for example, the review in Ref. 1). A large number of specific schemes for producing optically oriented states, which are found to be important in diverse phenomena, have been proposed and studied. In the most common cases the absorption of polarized resonance radiation and the subsequent spontaneous cascade transitions cause particles to flow between strongly and weakly absorbing magnetic sublevels and, consequently, enrich the weakly absorbing sublevels at the expense of the strongly absorbing sublevels.

Transitions in which the lower state is the ground state and the orientation of the ground state is studied are ordinarily considered. At the same time, a largely similar situation also occurs for excited states, specifically, metastable states, since “orientation” is accumulated in these states over a relatively long period of time. On the other hand, it must be emphasized that there is a fundamental difference between the optical orientation of the ground and metastable states. In the case of the ground state the process encompasses most atoms, and after optical excitation the atoms relax back into the initial, ground state. Formally, this means that under the given conditions the conservation of the number of particles plays an important role. As a rule, the relative number of atoms in metastable states is small. Only these atoms become involved in the optical-orientation process and the fraction of such particles is negligible in the overall particle balance. Moreover, after excitation the atoms do not necessarily return to the initial metastable state. Several relaxation channels could be important and the relative probabilities of the channels (the branching ratios) become important. In the case of metastables these circumstances make it possible to employ the classical kinetic model, typical for a small subsystem interacting with a thermostat.

In summary, optical orientation itself in the metastable and ground states has common physical origins. As will be shown below, however, the specific manifestations of optical orientation in these two cases can be radically different. Even the signs of the effects can be different.

In the present paper three types of phenomena are studied—orientation of metastable states by means of polarized radiation (Sec. 2), absorption of the orienting field (Sec. 3), and the absorption spectrum of the probe field with isotropic and anisotropic excitations (Secs. 4 and 5). A discussion of the results is given in Sec. 6.

2. OPTICAL ORIENTATION OF METASTABLE ATOMS

The metastable states are characterized by relatively slow relaxation, as a result of which saturation is strongly pronounced for transitions in which they participate, even at moderate radiation powers. For this reason, the interaction of metastable states with laser radiation is strongly nonlinear and relatively complicated, requiring that the scheme of the energy levels and the properties of the radiation be specified. For a number of reasons, we shall consider a transition between levels m, n with the same total angular momenta $J_m = J_n = 2$. The radiation is assumed to be a linearly polarized, monochromatic, plane wave (frequency ω , wave vector \mathbf{k}) resonant with the $m-n$ transition (the Bohr frequency is ω_{mn}). The gas pressure is assumed to be low enough so that the collisions can be neglected and relaxation is associated only with spontaneous transitions.

We choose a coordinate system with the quantization axis z oriented along the electric field vector \mathbf{E} of the wave. In this coordinate system the field \mathbf{E} induces transitions $\Delta M = 0$, represented in Fig. 1 by the solid arrows. The dashed arrows in Fig. 1 symbolize spontaneous transitions $mM \rightarrow nM + \Delta M$, where $\Delta M = 0, \pm 1$.

We introduce the following simplified notation for the

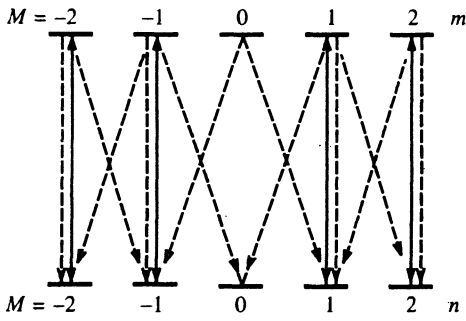


FIG. 1. Scheme of induced and spontaneous transitions between the degenerate lower and upper states of an atom ($J_m = J_n = 2$).

elements of the density matrix $\rho(jJ_n M, j'J_n M')$ in the stationary-state representation:

$$\rho(mJ_m M, mJ_m M) = r_M, \quad \rho(nJ_n M, nJ_n M) = \rho_M, \quad (2.1)$$

$$\begin{aligned} \rho(mJ_m M, mJ_m M') &= \rho_{MM'}^m, & \rho(nJ_n M, nJ_n M') &= \rho_{MM'}^n, \\ &= \rho_{MM'}^n, & & \end{aligned} \quad (2.2)$$

$$\rho(mJ_m M, nJ_n M') = \rho_{MM'} \quad (2.3)$$

The kinetic equations for the elements of the density matrix under stationary conditions have the form (see, for example, Refs. 2 and 3)

$$\begin{aligned} \Gamma_n \rho_M &= -W_M(\rho_M - r_M) + \sum_{M'} A_{MM'} r_{M'} + Q_M, \\ \Gamma_M r_M &= W_M(\rho_M - r_M) + q_M. \end{aligned} \quad (2.4)$$

Here the standard notation is used:

$$\begin{aligned} W_M &= \frac{2\Gamma |G_M|^2}{\Gamma^2 + \Omega_1^2}, & \Omega_1 &= \Omega - \mathbf{k} \cdot \mathbf{v}, & \Omega &= \omega - \omega_{mn}, \\ 2\Gamma &= \Gamma_m + \Gamma_n, & & & & \end{aligned} \quad (2.5)$$

$$G_M = (dE/2\sqrt{3}\hbar)(-1)^{J_n - M} \langle J_n M J_n - M | 10 \rangle. \quad (6)$$

Γ_m , Γ_n and q_M , Q_M are the relaxation rates and excitations of the sublevels mM , nM , \mathbf{v} is the velocity of the atom, d is the reduced dipole-moment matrix element for the $m-n$, transition, and $\langle \dots | \dots \rangle$ denotes a vector-addition coefficient. The sum on the right-hand side of the first equation in Eqs. (2.4) describes spontaneous cascade transitions $mM' \rightarrow nM$, whose rates are

$$A_{MM'} = A_{mn} \langle J_m M' 1 M - M' | J_n M \rangle^2, \quad M' = M, M \pm 1, \quad (2.7)$$

where A_{mn} is the first Einstein coefficient.

The relations (2.4)–(2.7) are valid for arbitrary values of J_m and J_n . For the case $J_m = J_n = 2$, which will be of special interest below, we have

$$\begin{aligned} A_{00} &= 0, & A_{10} &= A_{mn}/2, & A_{11} &= A_{mn}/6, \\ A_{21} &= A_{mn}/3, & A_{22} &= 2A_{mn}/3. \end{aligned} \quad (2.8)$$

The remaining quantities can be found with the aid of the relations

$$A_{MM'} = A_{M'M}, \quad A_{-M-M'} = A_{MM'}. \quad (2.9)$$

The quantities W_M are the rates of the induced transitions $mM \leftrightarrow nM$. Their values for $J_m = J_n$ are proportional to M^2 , specifically, $W_0 = 0$ and $W_2/w_1 = 4$. The sublevels $m0$ and $n0$ do not interact with an external field, and the spontaneous transitions $m1 \rightarrow n0$ lead to high occupancy of the sublevel $n0$. Indeed, we find from Eqs. (2.4)

$$r_0 = q_0/\Gamma_m, \quad \rho_0 = [Q_0 + A_{01}(r_1 + r_{-1})]/\Gamma_n. \quad (2.10)$$

The term proportional to A_{01} describes the particle flux into the sublevel $n0$, leading to orientation of the state n .

If the off-diagonal terms $A_{MM'} r_{M'}$ are dropped, then the system of equation (2.4) will describe the interaction of the four sublevels of the M subsystems ($M = \pm 1, \pm 2$), independent of one another, with the field. The determinants of the corresponding pairs of equations

$$\begin{aligned} \Delta_M &= \Gamma_m \Gamma_n + (\Gamma_m + \Gamma_n - A_{MM}) W_M = \Gamma_m \Gamma_n (\Gamma_{M_S}^2 \\ &+ \Omega_1^2) / (\Gamma^2 + \Omega_1^2), \\ \Gamma_{M_S}^2 &= \Gamma^2 [1 + (\Gamma_m + \Gamma_n - A_{MM}) \kappa_M / \Gamma_m], \\ \kappa_M &= 2|G_M|^2 / \Gamma \Gamma_n, \end{aligned} \quad (2.11)$$

determine the resonance properties of such M subsystems, Γ_{M_S} being the “saturated widths” of the subsystems. The spontaneous transitions $m1 \rightarrow n2$ and $m2 \rightarrow n1$ “couple” the two subsystems with $M = 1$ and 2 , and the system of equations is found to be of fourth order.

The excitation rates can depend on M . Such a dependence obtains in a gas discharge (self-alignment phenomenon^{4,5}), and it can strongly affect the absorption spectrum of the probe field (see Sec. 5). For this reason, we write out the general solution of Eqs. (4), assuming only a symmetric dependence of q_M and Q_M on M (i.e., $q_M = q_{-M}$, $Q_M = Q_{-M}$):

$$\begin{aligned} \rho_2 = \rho_{-2} &= \frac{1}{\Delta} \left\{ Q_2(\Gamma_m + W_2)\Delta_1 + Q_1 A_{21}(\Gamma_m + W_2)W_1 \right. \\ &+ q_2[(A_{22} + W_2)\Delta_1 + A_{12}^2 W_1] + q_1 A_{21}(\Gamma_m + W_2) \\ &\times (\Gamma_n + W_1) + q_0 \frac{A_{10}}{\Gamma_m} A_{21}(\Gamma_m + W_2)W_1 \left. \right\}, \end{aligned} \quad (2.12)$$

$$\begin{aligned} \rho_2 - r_2 &= \frac{1}{\Delta} \left\{ Q_2 \Gamma_m \Delta_1 + Q_1 \Gamma_m W_1 + q_2[(A_{22} - \Gamma_n)\Delta_1 \right. \\ &+ A_{12}^2 W_1] + q_1 A_{21}(\Gamma_n + W_1)\Gamma_m \\ &+ q_0 \frac{A_{10}}{\Gamma_m} A_{21} \Gamma_m W_1 \left. \right\}, \end{aligned} \quad (2.13)$$

$$\begin{aligned} \rho_1 = \rho_{-1} &= \frac{1}{\Delta} \left\{ Q_2 A_{12}(\Gamma_m + W_1)W_2 + Q_1(\Gamma_m + W_1)\Delta_2 \right. \\ &+ q_2 A_{12}(\Gamma_m + W_1)(\Gamma_n + W_2) + q_1 \left[(A_{11} + W_1)(\Delta_2 \right. \end{aligned}$$

$$+A_{21}^2 W_2] + q_0 \frac{A_{10}}{\Gamma_m} (\Gamma_m + W_1) \Delta_2 \Big\}, \quad (2.14)$$

$$\rho_1 - r_1 = \frac{1}{\Delta} \left\{ Q_2 A_{12} \Gamma_m W_2 + Q_1 \Delta_2 \Gamma_m + q_2 A_{12} (\Gamma_n + W_2) \Gamma_m + q_1 [(A_{11} - \Gamma_n) \Delta_2 + A_{21}^2 W_2] + q_0 \frac{A_{10}}{\Gamma_m} W_1 \Delta_2 \right\}. \quad (2.15)$$

Here we introduced the notation

$$\Delta = \Delta_1 \Delta_2 - A_{21} A_{12} W_1 W_2 \quad (2.16)$$

for the determinant of the system of four equations for ρ_2 , r_2 , ρ_1 , and r_1 .

Terms containing $A_{MM'}$, which describe the contributions of the cascade transitions $mM' - nM$ to ρ_M and r_M , appear in the expressions (2.10)–(2.16). We deliberately did not use the numerical values for $A_{MM'}/A_{mn}$ from Eq. (2.8) so as to be able to trace the origin of one or another term.

The following simple and physically obvious relations hold in the absence of an external field

$$\begin{aligned} \rho_2 &\equiv \rho_2^0 = \frac{1}{\Gamma_n} \left(Q_2 + \frac{1}{\Gamma_m} \sum_{M'} A_{2M'} q_{M'} \right), \\ \rho_1 &\equiv \rho_1^0 = \frac{1}{\Gamma_n} \left(Q_2 + \frac{1}{\Gamma_m} \sum_{M'} A_{1M'} q_{M'} \right), \\ \rho_0 &\equiv \rho_0^0 = \frac{1}{\Gamma_n} \left[Q_0 + 2 \frac{A_{01}}{\Gamma_m} q_1 \right], \quad r_M = r_M^0 = \frac{q_M}{\Gamma_m}. \end{aligned} \quad (2.17)$$

We now consider the expression for ρ_0 . We assume that $\Gamma_m \gg \Gamma_n$, and we drop terms of order Γ_n/Γ_m .

The case of high intensity, $W_M \gg \Gamma_m \gg \Gamma_n$, when ρ_M and r_M are virtually identical and ρ_0 can assume a large value on account of the optical pumping, is of interest for optical orientation:

$$\begin{aligned} \rho_0 &= \frac{1}{\Gamma_n} [Q_0 + 2a_2(Q_2 + q_2) + 2a_1(Q_1 + q_1) + a_0 q_0], \\ a_2 &= \frac{\alpha^2}{6-5\alpha}, \quad a_1 = \alpha \frac{3-2\alpha}{6-5\alpha}, \quad a_0 = \alpha^2 \frac{3-2\alpha}{6-5\alpha}, \end{aligned} \quad (2.18)$$

$$\alpha = A_{mn}/\Gamma_m.$$

The excess of ρ_0 above the value of the ratio Q_0/Γ_n , achieved by a direct excitation of the sublevel $n0$, depends critically on the branching ratio α , which determines the fraction of the rate of the “useful” transition A_{mn} with respect to the total decay rate Γ_m of the level m to all levels. If $\alpha = A_{mn}/\Gamma_m = 1$, then it follows from Eq. (2.18) that

$$\rho_0 = \frac{1}{\Gamma_n} \sum_M (Q_M + q_M), \quad (2.19)$$

i.e. all events of excitation of all sublevels mM and nM lead to filling of the sublevel $n0$. This result, which is valid up to terms of order Γ_n/Γ_m which have been dropped, is obvious and in some sense makes the optical pumping of the ground state and of the metastable atom closer. However, even if

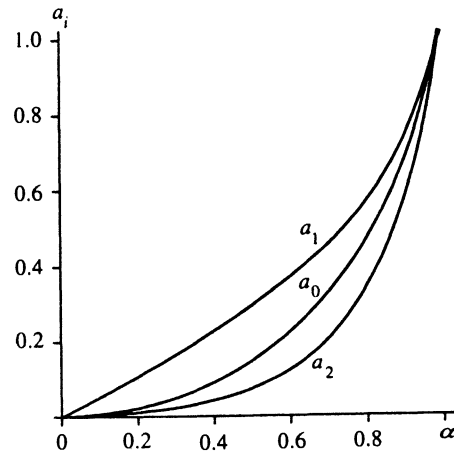


FIG. 2. a_2 , a_1 and a_0 versus the branching ratio α .

ω does not differ much from 1, the value of ρ_0 drops sharply. Figure 2 displays plots of the factors a_2 , a_1 , and a_0 , which according to the relation (2.18) determine the contribution of $Q_2 + q_2$, $Q_1 + q_1$, and q_0 , respectively, to ρ_0 . All three factors decrease approximately by a factor of 2 even for $1 - \alpha = 0.15$ and reach the value 0.1 for $\alpha = 0.6, 0.2$, and 0.45, respectively.

For small values of α the factor a_1 depends linearly on α , and the factors a_2 and a_0 depend quadratically on α . This is how it should be: The atom can pass from the states $m1$ and $n1$ into the level $n0$ as a result of a spontaneous transition and there must be a linear dependence on α ; an atom can pass from $m2$ and $n2$ into $n0$ after two successive spontaneous transitions, and for this reason the dependence on α should be quadratic. Since the direct $m0 - n0$ transition is forbidden, an atom passes into the state $n0$ from the state $m0$ also as a result of two spontaneous transitions.

The foregoing arguments are valid for any values $J_m = J_n$: The contribution of the excitation rates $Q_M + q_M$ to the occupancy of the sublevel $n0$ for small values of α will be proportional to α^M ($M \geq 1$) and the highest power will be α^{J_m} .

Therefore the efficiency of optical pumping drops rapidly for comparatively low values of $1 - \alpha = 0.1 - 0.15$. This result is due to the “wandering” of the atom through the magnetic sublevels nM as a result of the spontaneous transitions $mM \rightarrow nM$ and $mM \rightarrow nM \pm 1$ and departure of the atom via the channels $m \rightarrow j \neq n$. Qualitatively, this result also pertains to transitions between levels with different values of $J_m, J_n \neq 2$.

We shall study first the dependence of ρ_0 on the intensity of the field for $\Omega_1 = 0$ and isotropic excitation (Q_M and q_M do not depend on M). Under these conditions, we find from Eqs. (2.10), (2.15), (2.17), and (2.18)

$$\begin{aligned} \chi &= \frac{\rho_0 - \rho_0^0}{\rho_0^0 - r^0} = \frac{\alpha}{4} \frac{[1 + 4(1 - \alpha/3)\kappa]\kappa}{1 + 5(1 - 17\alpha/30)\kappa + 4(1 - 5\alpha/6)\kappa^2}, \\ \rho^0 - r^0 &\equiv \rho_1^0 - r_1^0 = \rho_2^0 - r_2^0, \quad \kappa \equiv \kappa_1. \end{aligned} \quad (2.20)$$

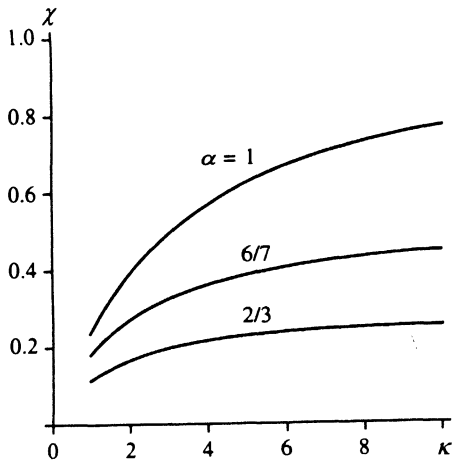


FIG. 3. Occupancies of the sublevel $M=0$ of the metastable state of an atom as a function of the intensity of the orienting field.

According to this expression, the occupancy of the sublevel $n0$ as a function of the field intensity (κ) has the form of curves with "saturation" (see Fig. 3). In accordance with Fig. 2, the asymptotic values (in the limit $\kappa \rightarrow \infty$) drop rapidly as α decreases, even for small $1 - \alpha$. The rate at which the asymptotic limit is reached decreases as $\alpha \rightarrow 1$. This is also seen from Eq. (2.20): The coefficient of κ^2 in the denominator decreases as α increases.

In contrast to saturation in a two-level model, the curves in Fig. 3 are described by an expression in which the numerator and denominator are quadratic functions of the intensity. This fact is closely associated with the optical pumping, because it is due precisely to the spontaneous cascade transitions $mM \rightarrow nM \pm 1$. In the general case, the exponent of the terms which are of highest order in the intensity will be equal to the angular momentum J_m of the levels. Indeed, atoms excited into the "extreme" sublevel $M=J_m$ reach the sublevel $n0$ as a result of alternating absorption $nM \rightarrow mM$ and spontaneous emission $mM \rightarrow nM - 1$ events. There are J_m such transition pairs. The terms of highest order in the intensity will contain the product

$$\prod_{M=1}^{J_m} \kappa_M,$$

i.e., the intensity will appear to the power J_m .

The expression (2.20) gives the maximum value of ρ_0 achieved with $\Omega_1=0$. Since $\Omega_1 = \omega - \omega_{mn} - \mathbf{k} \cdot \mathbf{v}$, the dependence on Ω_1 can be regarded as a dependence on the projection of \mathbf{v} on the wave vector \mathbf{k} . Aside from Ω_1 , q_M and Q_M also depend on \mathbf{v} , for example, in accordance with a Maxwellian distribution. We assume, for simplicity, that the excitation is isotropic. In this case, it follows from Eqs. (2.10) and (2.15) that

$$\rho_0 = \rho_0^0 + \alpha \kappa \frac{\Gamma^2(\Gamma_3^2 + \Omega_1^2)}{(\Gamma_1^2 + \Omega_1^2)(\Gamma_2^2 + \Omega_1^2)} (\rho^0 - r^0)$$

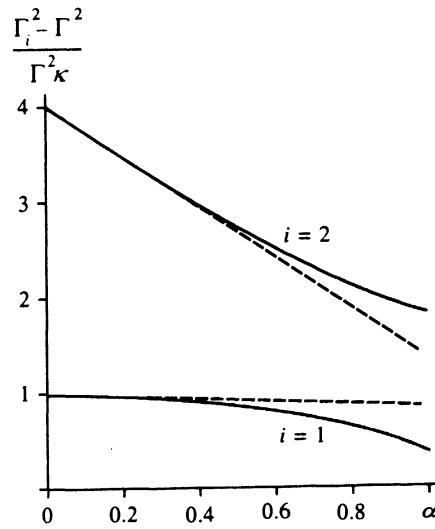


FIG. 4. Γ_1 and Γ_2 versus α with optical pumping (solid lines) and without optical pumping (dashed lines).

$$= \rho_0^0 + \alpha \kappa \left[\frac{\Gamma_1^2 A_1}{\Gamma_1^2 + \Omega_1^2} - \frac{\Gamma_2^2 A_2}{\Gamma_2^2 + \Omega_1^2} \right] (\rho^0 - r^0), \quad (2.21)$$

where

$$\begin{aligned} \Gamma_1^2 &= \Gamma^2 \{ 1 + [1 - \alpha/6 - (\mathcal{D} - B)] \kappa \} \\ &= \Gamma^2 \left\{ 1 + \left[\frac{5}{2} \left(1 - \frac{17}{30} \alpha \right) - \mathcal{D} \right] \kappa \right\}. \end{aligned} \quad (2.22)$$

$$\begin{aligned} \Gamma_2^2 &= \Gamma^2 \{ 1 + [4(1 - 2\alpha/3) + \mathcal{D} - B] \kappa \} \\ &= \Gamma^2 \left\{ 1 + \left[\frac{5}{2} \left(1 - \frac{17}{30} \alpha \right) + \mathcal{D} \right] \kappa \right\}, \end{aligned} \quad (2.23)$$

$$B = \frac{3}{2} \left(1 - \frac{5}{6} \alpha \right), \quad \mathcal{D} = \sqrt{B^2 + \left(\frac{2}{3} \alpha \right)^2}, \quad \kappa \equiv \kappa_1, \quad (2.24)$$

$$\begin{aligned} \Gamma_3^2 &= \Gamma^2 \{ 1 + 4(1 - \alpha/3) \kappa \} \\ A_1 &= (1 + A) \Gamma^2 / \Gamma_1^2, \quad A_2 = A \Gamma^2 / \Gamma_2^2, \\ A &= \left(\frac{4}{3} \alpha + B - \mathcal{D} \right) / 2\mathcal{D}. \end{aligned} \quad (2.25)$$

Therefore the dependence of ρ_0 on Ω_1 (or on \mathbf{v}) is described by two Lorentzian curves with half-widths Γ_1 and Γ_2 . The Lorentzians have different signs: Since $4\alpha/3 + B > \mathcal{D}$ and therefore $A > 0$, the term with the width Γ_2 is "negative." Incidentally, it plays a comparatively small role: The ratio of its amplitude A_2 to the amplitude A_1 of the first Lorentzian is equal to 1/13 for $\alpha=1$ and decreases as α decreases.

For small values of α , we have $\mathcal{D} \approx B$ up to terms of order α , and the half-widths Γ_1 and Γ_2 are approximately equal to the saturation widths Γ_{1S} and Γ_{2S} for the transitions $m1 - n1$ and $m2 - n2$, respectively, in the absence of coupling between them. The dashed lines in Fig. 4 display Γ_1^2 and Γ_2^2 as a function of α in this approximation. The terms

$\mathcal{S}-B$ are found to be important for $\alpha > 1/2$ and, especially, near the point $\alpha = 1$. In the region $1 - \alpha \ll 1$ we have

$$\mathcal{S} \approx \frac{\sqrt{73}}{12} - \frac{19}{12\sqrt{73}}(1 - \alpha),$$

$$\Gamma_1^2 \approx \Gamma^2 \{1 + [0.37 + 1.60(1 - \alpha)]\kappa\} \quad (2.26)$$

$$\Gamma_2^2 \approx \Gamma^2 \{1 + [1.80 + 1.23(1 - \alpha)]\kappa\}. \quad (2.27)$$

We underscore the fact that for $1 - \alpha \ll 1$ the half-widths Γ_1 are much smaller than the half-width $\Gamma^2[1 + (1 - \alpha/6)\kappa]$ (dashed line in Fig. 4).

The combination $(\Gamma_1^2 + \Omega_1^2)(\Gamma_2^2 + \Omega_2^2)$ is proportional to the determinant Δ of the system of equations (2.4) and appears in all expressions (2.12)–(2.15) for ρ_M and r_M . Therefore similar resonances with the half-widths Γ_1 and Γ_2 will be present in the velocity distributions of ρ_M and r_M ($M=1$ and 2 , the Bennett structure). For example,

$$\rho_1 - r_1 = \frac{(\Gamma_3^2 + \Omega_1^2)(\Gamma^2 + \Omega_1^2)}{(\Gamma_1^2 + \Omega_1^2)(\Gamma_2^2 + \Omega_1^2)}, \quad (2.28)$$

$$\rho_2 - r_2 = \frac{(\Gamma_4^2 + \Omega_1^2)(\Gamma^2 + \Omega_1^2)}{(\Gamma_1^2 + \Omega_1^2)(\Gamma_2^2 + \Omega_1^2)}, \quad (2.29)$$

$$\Gamma_4^2 = \Gamma^2 [1 + (1 + \alpha/6)\kappa].$$

Such structures will arise on the depleted and enriched magnetic sublevels for other values of J_m and J_n also, the number of Lorentzians, their amplitude and half-widths depending on J_m , J_n , and the polarization and intensity of the field.

3. ABSORPTION OF THE ORIENTING FIELD

The general expression for the absorbed power has the form

$$P = -2\hbar\omega \operatorname{Re} \left\langle i \sum_{MM'} \rho(mJ_m M, nJ_n M') G_{MM'}^* \exp(i\Omega t) \right\rangle, \quad (3.1)$$

$$G_{MM'} = \frac{1}{\sqrt{3}} d \sum_{\sigma} (-1)^{J_n - M'} \langle J_n M J_n - M' | 1\sigma \rangle E_{\sigma}, \quad (3.2)$$

where E_{σ} is the circular component of \mathbf{E} and the brackets in Eq. (3) denote averaging over the velocities \mathbf{v} . Using the notation introduced above, we can write in our case of a linearly polarized field

$$\begin{aligned} P &= 2\hbar\omega \langle W_1(\rho_1 - r_1) + W_2(\rho_2 - r_2) \rangle \\ &= \left\langle \frac{2\hbar\omega\Gamma^2\Gamma_n}{(\Gamma_1^2 + \Omega^2)(\Gamma_2^2 + \Omega^2)} [\kappa_1(\Gamma_3^2 + \Omega^2) + \kappa_2(\Gamma_4^2 + \Omega^2)] \right. \\ &\quad \left. \times (\rho^0 - r^0) \right\rangle. \end{aligned} \quad (3.3)$$

We perform the averaging over the velocities under the assumption that the distributions $\rho_M^0 - r_M^0$ are Maxwellian:

$$\rho_M^0 - r_M^0 = (\bar{\rho}_M - \bar{r}_M) (\sqrt{\pi}\bar{v})^{-3} \exp(-v^2/\bar{v}^2),$$

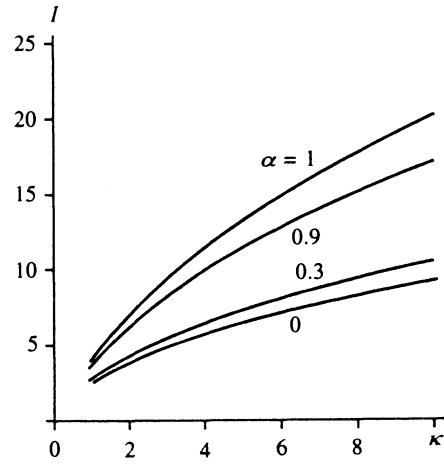


FIG. 5. Absorption of the field as a function of its intensity for $\alpha = 1, 0.9, 0.3$, and 0 .

$$\bar{v}^2 = 2T/m_0, \quad (3.4)$$

where $\bar{\rho}_M$ and \bar{r}_M are the populations of the sublevels nM and mM integrated over \mathbf{v} . In the limit

$$k\bar{v} \gg \Gamma_1, \Gamma_2 \quad (3.5)$$

we arrive at the relations

$$\begin{aligned} P &= \hbar\omega \frac{2\sqrt{\pi}}{k\bar{v}} \exp\left[-\frac{\Omega^2}{(k\bar{v})^2}\right] \Gamma_n \Gamma(\bar{\rho}^0 - \bar{r}^0) I, \\ \Omega &= \omega - \omega_{mn}, \end{aligned} \quad (3.6)$$

$$I = \frac{\Gamma}{\Gamma_1 + \Gamma_2} \left\{ \left(1 + \frac{\Gamma_3^2}{\Gamma_1\Gamma_2}\right) \kappa_1 + \left(1 + \frac{\Gamma_4^2}{\Gamma_1\Gamma_2}\right) \kappa_2 \right\}. \quad (3.7)$$

In Eq. (3.7) the terms proportional to κ_1 and κ_2 determine the absorption on the transitions $n1 - m1$ and $n2 - m2$, respectively. Taking into consideration the equality $\kappa_2 = 4\kappa_1$ and the expressions (2.24) and (2.29) for Γ_3 and Γ_4 , we obtain

$$I = \frac{5\Gamma\kappa}{\Gamma_1 + \Gamma_2} \left\{ 1 + \frac{\Gamma^2}{\Gamma_1\Gamma_2} \left[1 + \frac{8}{5} \left(1 - \frac{\alpha}{12}\right) \kappa \right] \right\}, \quad \kappa \equiv \kappa_1. \quad (3.8)$$

Plots of I as a function κ for $\alpha = 1, 0.9, 0.3$, and 0 are displayed in Fig. 5. Just as for a Doppler-broadened line in the two-level model, after the linear section for small values of κ , the function I approaches the asymptotic behavior $I \propto \sqrt{\kappa}$ for $\kappa \gg 1$ (as long as, of course, the condition (3.5) holds or $\kappa \ll kv/\Gamma_{1,2}$). In this asymptotic region the coefficient of $\sqrt{\kappa}$ depends strongly on α , increasing with α (Fig. 6), and most rapidly near the point $\alpha = 1$. The latter property is due mainly to the factor $1/\Gamma_1\Gamma_2$ in Eq. (3.8). As α increases from 0 to 1 , the quantity $I/\sqrt{\kappa}$ increases by a factor of 2.35 .

We emphasize that this increase of the absorption of power with increasing α occurs for a fixed value of the unsaturated absorption coefficient, i.e., it is due to the influence of cascades on the nonlinear absorption. We recall that in the

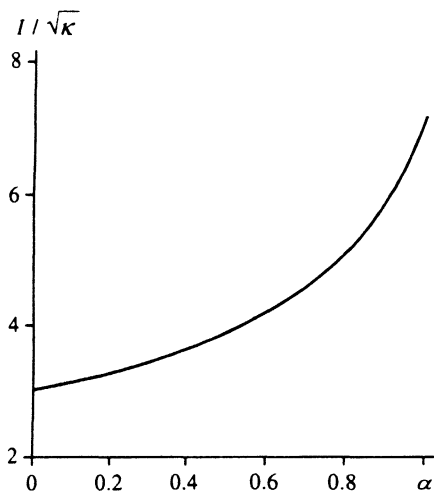


FIG. 6. Absorption of the field versus α for an intense field ($\kappa_1 \gg 1$).

two-level model the saturation factor has the form $(1 - \alpha)\kappa$ and vanishes at $\alpha = 1$, i.e., the absorption coefficient does not saturate at all. Therefore the degeneracy of the levels and the existence of spontaneous transitions with $\Delta M = \pm 1$ decrease the role of cascades in saturation.

Analysis of the determinant of the system of equations (4) shows that as the angular momenta J_m and J_n of the levels increases, the behavior of the plot in Fig. 6 becomes increasingly sharper near the point $\alpha = 1$. The physical explanation was already mentioned above: As J_m increases, the number of magnetic sublevels increases as the role of the migration of atoms over the sublevels increases. For this reason, the introduction of relaxation to the third levels with large J_m will have a stronger effect.

4. ABSORPTION SPECTRUM OF THE PROBE FIELD

It is well known that probe-field spectroscopy is a powerful method for investigating the most diverse radiation and kinetic processes (see, for example, Refs. 2, 3, and 6). The optical orientation and the long lifetime of metastable atoms introduce fundamentally new effects if the total angular momentum $J_n \geq 2$. For this reason, we shall study the simplest case $J_n = 2$ (in the collisionless model, as in Secs. 2 and 3).

Let the probe field \mathbf{E}_2 be a monochromatic plane wave (frequency ω_2 , wave vector \mathbf{k}_2), polarized linearly and orthogonally to the orienting field \mathbf{E}_1 (frequency ω_1 , wave vector \mathbf{k}_1). The power P_2 absorbed from the probe field is given by the general expression

$$P_2 = -2\hbar\omega_2 \operatorname{Re} \left\langle \sum_{MM'} i\rho_{MM'} g_{MM'}^* \exp(i\Omega_2 t) \right\rangle, \quad (4.1)$$

where $\rho_{MM'}$ are determined by Eq. (2.3), and

$$g_{MM'} = \frac{d}{2\sqrt{3}\hbar} \sum_{\sigma} (-1)^{J_n - M'} \langle J_n M J_n - M' | 1 \sigma \rangle E_{2\sigma},$$

$$\sigma = \pm 1, \quad \Omega_2 = \omega_2 - \omega_{mn} - k_2 v. \quad (4.2)$$

The matrix elements $g_{MM'}$ are different from 0 for $|M' - M| = |\sigma| = 1$ and are equal to ($J_m = J_n = 2$)

$$g_{01} = g/\sqrt{2}, \quad g_{12} = g/\sqrt{3},$$

$$g_{MM'} = -g_{M'M} = g_{-M-M'}, \quad g = \frac{dE_2}{2\sqrt{6}\hbar} \quad (4.3)$$

The equations for $\rho_{MM'}$ have the form

$$\dot{\rho}_{MM'} + \Gamma \rho_{MM'} = i(G_M \rho_{MM'}^n - \rho_{MM'}^m G_{M'}) \exp(-i\Omega_1 t)$$

$$+ i g_{MM'} (\rho_{M'} - r_M) \exp(-i\Omega_2 t)$$

$$+ i (g_{M2M-M'} \rho_{2M-M'M'}^n$$

$$- \rho_{M2M'-M}^m g_{2M'-MM'}) \exp(-i\Omega_2 t). \quad (4.4)$$

Here $\rho_{M'}$ and r_M are the occupancies of the sublevels nM' and mM , which can be found with the aid of Eqs. (2.10)–(2.16). The quantities $\rho_{MM'}^j$ ($j = m, n$) and $\rho_{2M-M'M'}^n$, $\rho_{M2M'-M}^m$ describe the correlation between the magnetic sublevels of the same level, the differences of the magnetic quantum numbers being

$$M - M' = \pm 1, \quad (2M - M') - M' = \pm 2,$$

$$(2M' - M) - M = \mp 2.$$

It is evident from the relation (4.1) that the components $\rho_{MM'}$, oscillating with frequency Ω_2 according to the law

$$\rho_{MM'} = \bar{\rho}_{MM'} \exp(-i\Omega_2 t). \quad (4.5)$$

make a stationary contribution to P_2 . According to Eqs. (4.4), the stationary populations $\rho_{M'}$ and r_M and the stationary correlations between the magnetic sublevels with magnetic quantum numbers differing by ± 2 give such a dependence. The quantities $\rho_{MM'}^j$, however, should oscillate with the difference frequency

$$\Omega_1 - \Omega_2 = \omega_1 - \omega_2 - (k_1 - k_2)v. \quad (4.6)$$

If the orienting and probe fields are parallel to one another, then we have $\mathbf{k}_1 \approx \mathbf{k}_2$, the frequency difference (4.6) is virtually independent of v , atoms with all velocities will participate in the corresponding radiation process, and the terms $\rho_{MM'}^j$ will be real. Nonlinear interference effects (NIE) will play a large role in this case.^{2,3} In the case of oppositely directed waves ($\mathbf{k}_1 \approx -\mathbf{k}_2$) the elements $\rho_{MM'}^j$ oscillate rapidly for most atoms, and the nonlinear interference effects should be small. These properties of the nonlinear interference effects are well known in probe-field spectroscopy in three-level systems.^{2,3,6}

In the present paper we are considering the case of oppositely directed waves, when nonlinear interference effects are not important. We write instead of Eqs. (4.4),

$$(\Gamma - i\Omega_2) \bar{\rho}_{MM'} = i g_{MM'} (\rho_{M'} - r_M)$$

$$+ i (g_{M2M-M'} \rho_{2M-M'M'}^n$$

$$- \rho_{M2M'-M}^m g_{2M'-MM'}) \quad (4.7)$$

The correlations of $\rho_{2M-M'M'}^n$ and $\rho_{M2M'-M}^m$ can appear as a result of excitation anisotropy and effects which are nonlinear in the probe-field intensity. For example, the equation for $\rho_{M2M'-M}^m$ has the form

$$\begin{aligned} \dot{\rho}_{M2M'-M}^m + \Gamma_m \rho_{M2M'-M}^m &= q_{M2M'-M} + iG_M \rho_{2M'-MM}^* \\ &\times \exp(-i\Omega_1 t) - i\rho_{M2M'-M} G_{2M'-m}^* \\ &\times \exp(i\Omega_1 t) + i g_{MM'} \rho_{2M'-MM'}^* \\ &\times \exp(-i\Omega_2 t) - i\rho_{MM'} g_{2M'-MM'}^* \exp(i\Omega_2 t). \end{aligned} \quad (4.8)$$

The last two terms on the right-hand side of Eq. (4.8) are proportional to $|g|^2$, and as can be seen from Eqs. (4.1) and (4.7), they make a contribution of order $|g|^4$ to P_2 [terms which make a contribution of order $|g|^6$ to P_2 are dropped in Eq. (4.8)]. In the case of anisotropic excitation $q_{M2M'-M} \neq 0$, and this term makes a contribution of order $|g|^2$ to P_2 . The terms in Eq. (4.8) which contain the amplitude of the orienting field (G_M , $G_{2M'-M}^*$) couple $\rho_{M2M'-M}^m$ with the off-diagonal elements $\rho_{2M'-MM}$ and $\rho_{M2M'-M}$ of the density matrix on the forbidden transitions.

We consider first the simplest case: isotropic excitation ($q_{M2M'-M} = 0$) and linear (in $|g|^2$) absorption of the probe field. For these conditions

$$\bar{\rho}_{MM'} = i g_{MM'} (\rho_{M'} - r_{M'}) / (\Gamma - i\Omega_2). \quad (4.9)$$

Keeping in mind the relation (4.3) and the relations $\rho_M = \rho_{-M}$, $r_m = -r_{-m}$, we arrive at the formulas

$$P_2 = 2\hbar\omega |g|^2 \left\langle \frac{\Gamma}{\Gamma^2 + \Omega_2^2} N(\Omega_1) \right\rangle, \quad (4.10)$$

$$N(\Omega_1) = \rho_0 - r_0 + \frac{5}{3} (\rho_1 - r_1) + \frac{2}{3} (\rho_2 - r_2). \quad (4.11)$$

The quantity $N(\Omega_1)$ can be interpreted as the effective population difference determining the absorption (or amplification) of the probe field. The difference $\rho_1 - r_1$ has the greatest weight. This explained by the numerical values of $g_{MM'}$ and the number of transitions from different sublevels: four transitions $n \pm 1 \rightarrow m0$, ± 2 from the sublevels $M = \pm 1$ are possible, while two transitions $n0 \rightarrow m \pm 1$, $n \pm 2 \rightarrow m \pm 1$, ± 2 are possible from the sublevels $M = 0$ and $M = \pm 2$. According to Eqs. (2.21), (2.28), and (2.29), $N(\Omega_1)$ can be represented as a linear combination of two Lorentzians with the half-widths Γ_1 and Γ_2 :

$$N(\Omega_1) = \frac{10}{3} \left[1 + \frac{\Gamma_1^2 B_1}{\Gamma_1^2 + \Omega_1^2} + \frac{\Gamma_2^2 B_2}{\Gamma_2^2 + \Omega_1^2} \right] (\rho_1^0 - r_1^0). \quad (4.12)$$

As soon as $\Gamma_1, \Gamma_2 \ll k\bar{v}$, $N(\Omega_1)$ as a function of $\mathbf{k}_1 \cdot \mathbf{v}$ exhibits a sharp (on the scale $k\bar{v}$) structure (similar to the Bennett's structure), formed by the orienting field superposed on the the Maxwellian distribution.

The relative amplitude of the sharp structure is described by the expression

$$H = B_1 + B_2 = (3\alpha\kappa\Gamma^2\Gamma_3^2 + 5\Gamma^2\Gamma_3^2 + 2\Gamma^2\Gamma_4^2)$$

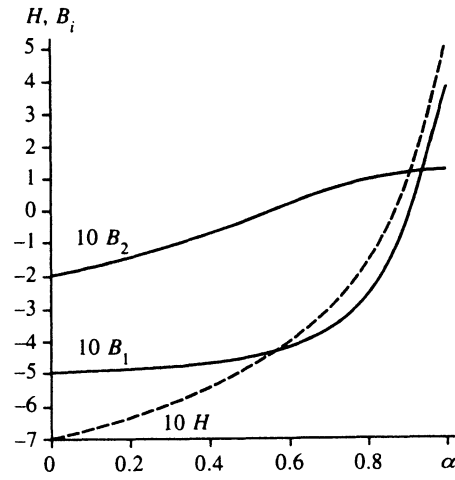


FIG. 7. Behavior of the amplitude (H) of the total probe-field absorption peak and its components (B_1, B_2) as a function of α for a high intensity of the orienting field ($\kappa \gg 1$).

$$-7\Gamma_1^2\Gamma_2^2/10\Gamma_1^2\Gamma_2^2. \quad (4.13)$$

Substituting here the values of Γ^2 from Eqs. (2.22)–(2.24) and (2.29), we find

$$H = \frac{\kappa}{4} \frac{1 - \frac{33}{5}(1-\alpha) + \frac{4}{3} \left[1 - \frac{41}{5}(1-\alpha) - \frac{6}{5}(1-\alpha)^2 \right] \kappa}{1 + \frac{13}{6} \left[1 + \frac{17}{13}(1-\alpha) \right] \kappa + \frac{2}{3} [1 + 5(1-\alpha)] \kappa^2}. \quad (4.14)$$

For $\alpha = 1$ we have

$$H = \frac{\kappa}{4} \frac{1 + 4\kappa/3}{1 + 13\kappa/6 + 2\kappa^2/3}. \quad (4.15)$$

Therefore, in the present case we have $H > 0$ and the effective population difference $N(\Omega_1)$ contains a peak whose amplitude increases with the intensity of the field and reaches the value $1/2$ for $\kappa \gg 1$. In other words, the maximum amplitude of the peak is at most one-half of the unsaturated Maxwellian distribution. As $1 - \alpha$ increases, the amplitude of the peak decreases (see Fig. 7) and becomes negative at $1 - \alpha \approx 1/8$, i.e. the sharp structure becomes a dip whose depth increases with $1 - \alpha$ (and κ). The asymptotic value of H for $\alpha = 0$ and $\kappa \gg 1$ is $H = -0.7$.

The above-described behavior of H as a function of α and κ is evidently explained by the competition between the Bennett peak on the sublevel $n0$ and the Bennett dips in the population differences $\rho_M - r_M$ ($M = 1, 2$). For $\alpha = 1$ the optical pumping of the sublevel $n0$ is stronger than the depletion of the sublevels $M = \pm 1$ and ± 2 . As the branching ratio α decreases, an increasingly larger number of atoms escape into the third levels and do not reach the state $n0$.

Just as for other characteristics considered above, the amplitude H depends sharply on α for small values of $1 - \alpha$. This is illustrated well in Fig. 7 and by the formula (4.14), where large numerical coefficients appear in the terms with $1 - \alpha$. This property is associated with the small values

of the ratios $A_{MM'}/A_{mn}$ and repeated spontaneous transitions in the course of the migration of the atom to the state $n0$. The existence of relaxation to the third levels sharply increases the relative rate at which atoms leave the system of levels mM, nM .

The quantity H describes the amplitude of the total structure consisting of two Lorentzians with the half-widths Γ_1 and Γ_2 . The values of Γ_1 and Γ_2 do not differ very much (the ratio Γ_2/Γ_1 is at most 2.2, which is reached for $\alpha=1$ and $\kappa \gg 1$). Nonetheless, the amplitudes B_1 and B_2 of the Lorentzians are of interest in themselves. It follows (for isotropic excitation) from the expressions (2.17), (2.21), (2.28), and (2.29) for ρ_M and r_M that

$$B_1 = \frac{1}{10} \frac{\gamma_1 \kappa}{1 + \gamma_1 \kappa} \frac{1}{\gamma_2 - \gamma_1} [3\alpha(\gamma_3 - \gamma_1)/\gamma_1 - 5(\gamma_3 - \gamma_1) - 2(\gamma_4 - \gamma_1)], \quad (4.16)$$

$$B_2 = \frac{1}{10} \frac{\gamma_2 \kappa}{1 + \gamma_2 \kappa} \frac{1}{\gamma_2 - \gamma_1} [3\alpha(\gamma_3 - \gamma_2)/\gamma_2 - 5(\gamma_3 - \gamma_2) - 2(\gamma_4 - \gamma_2)], \quad (4.17)$$

where we have introduced the notation

$$\gamma_i \equiv (\Gamma_i^2 - \Gamma^2)/\Gamma^2 \kappa, \quad i = 1, 2, 3, 4, \quad (4.18)$$

which depend on α but not on κ . The amplitudes B_1 and B_2 increase with κ , and for $\gamma_1 \kappa \gg 1$ and $\gamma_2 \kappa \gg 1$ they reach asymptotic values, whose dependence on α is shown in Fig. 7. One can see that B_1 and B_2 change sign, which reflects the competition of the Bennett peaks and dips noted above for $\rho_0 - r_0$ and $\rho_1 - r_1, \rho_2 - r_2$. Over most of the range of values of α , the Lorentzian with the half-width Γ_1 plays the main role and $|B_1| = B_2$ occurs only near $\alpha = 0.9$. We note that for $0 < \alpha < 0.6$ the amplitudes B_1 and B_2 have the same sign (they are negative). The sharpness of the α dependence of H near the point $\alpha = 1$ is due to the term B_1 .

Averaging P_2 over \mathbf{v} (with a Maxwellian weight) under the condition (3.5) of large Doppler broadening gives the relations

$$P_2 = 2\hbar\omega_2 g^2 \frac{\sqrt{\pi}}{k\bar{v}} \exp[-(\Omega/k\bar{v})^2] \frac{10}{3} [1 + H_1(\Omega)] (\rho_1^0 - r_1^0), \quad (4.19)$$

$$H_1(\Omega) = \frac{\Gamma_1 B_1}{\Gamma_1 + \Gamma} \frac{(\Gamma_1 + \Gamma)^2}{(\Gamma_1 + \Gamma)^2 + (2\Omega)^2} + \frac{\Gamma_2 B_2}{\Gamma_2 + \Gamma} \frac{(\Gamma_2 + \Gamma)^2}{(\Gamma_2 + \Gamma)^2 + (2\Omega)^2}, \quad \Omega = (\omega_1 + \omega_2)/2. \quad (4.20)$$

Therefore the Ω dependence of P_2 has the form of two Lorentzians with half-widths $(\Gamma_1 + \Gamma)/2$ and $(\Gamma_2 + \Gamma)/2$. The relative amplitude of the spectral structure $H_1(0)$,

$$H_1(0) = \frac{\Gamma_1}{\Gamma_1 + \Gamma} B_1 + \frac{\Gamma_2}{\Gamma_2 + \Gamma} B_2, \quad (4.21)$$

for small κ is found to be two times smaller than H (if $\kappa \ll 1$, then $\Gamma_1 \approx \Gamma_2 \approx \Gamma$), while for $\kappa \gg 1$ we have Γ_1, Γ_2

$\gg \Gamma$ and $H_1(0) \approx H$. Therefore the structure of the absorption spectrum P_2 of the probe field and the velocity distribution of $N(\Omega_1)$ are virtually identical.

It is completely obvious that qualitatively the conclusions drawn above remain valid for arbitrary values of the total angular momentum J_n . The Bennett structure (and the structure of the absorption spectrum of the probe field) will consist of J_n Lorentzians with half-widths on the order of the half-width of the saturation in the $M-M$ transition

$$\Gamma_M^2 \approx \Gamma [1 + (1 - A_{MM}/\Gamma_m) \kappa M].$$

The total relative amplitude of the peak (dip) in the velocity distribution and in the absorption spectrum will increase with κ and will decrease rapidly as a function of α away from the point $\alpha = 1$.

Changing the polarization of the probe field \mathbf{E}_2 from the linear, orthogonal polarization of the orienting field \mathbf{E}_1 studied above will result in a decrease of H . Indeed, adding a z component to \mathbf{E}_2 will give rise to transitions with $\Delta M = 0$, which are allowed only for $M = \pm 1$ and ± 2 . As a result, the role of the differences $\rho_1 - r_1$ and $\rho_2 - r_2$ will increase. The latter differences are associated with the Bennett dips, and for this reason the relative role of the optical pumping should decrease. For example, the effective population difference for a circularly polarized probe field is proportional to

$$(\rho_0 - r_0) + \frac{7}{3} (\rho_1 - r_1) + \frac{10}{3} (\rho_2 - r_2)$$

[compare to the expression (4.11)], and as a simple analysis shows, this quantity is always negative, even for $\alpha = 1$. In other words, the absorption spectrum of a circularly polarized probe field should contain a structure in the form of a dip superposed on a Doppler-broadened line.

The theoretical results obtained above disagree sharply with the experimental results obtained by Kartashov and one of the present authors.⁷ In Ref. 7 powerful linearly polarized radiation from a one-frequency dye laser passed through a gas-discharge tube with neon (Ne^{20}). The frequency of the laser radiation was close to the Bohr frequency of the transition $1s_5(2p^5 3s[3/2]_2^0) - 2p_8(2p^5 3p[5/2]_2)$, $\lambda = 6334.4 \text{ \AA}$. This radiation served as the orienting radiation. The oppositely propagating probe field was produced by splitting off part of the laser beam mentioned above and changing its polarization into circular polarization (with the aid of a $\lambda/4$ plate). The power of the orienting fields was varied from 0 to $I_1 = 0.5 \text{ W/cm}^2$, which corresponds to $|G_1| = 4.9 \cdot 10^7 \text{ s}^{-1} = 7.8 \text{ MHz}$. The power of the probe field remained constant and equal to $I_2 = 10^{-4} \text{ W/cm}^2$, $|g| = 4.9 \cdot 10^5 \text{ s}^{-1} = 0.08 \text{ MHz}$. The numerical values of the radiation parameters of the transition were taken from Ref. 8 (p. 311):

$$A_{mn} = 1.36 \cdot 10^7 \text{ s}^{-1}, \quad \Gamma_m = 4.05 \cdot 10^7 \text{ s}^{-1},$$

$$\alpha = 0.336, \quad \Gamma = 2 \cdot 10^7 \text{ s}^{-1}.$$

The decay rate Γ_n of the lower metastable state $1s_5$ is determined by collisions with atoms and electrons in the gas-discharge plasma, and under the conditions of Ref. 7 $\Gamma_n \sim 10^9 \text{ s}^{-1}$. For this value of Γ_n and taking $I_1 = 0.1 \text{ W/cm}^2$, κ had the value

$$\kappa = 2|G_1|^2/\Gamma\Gamma_n = 500.$$

The absorption spectrum of the probe field recorded in Ref. 7 consisted of a superposition of a wide contour (with a width of order the Doppler width $k\bar{v} \approx 800$ MHz) and a comparatively sharp peak with a half-width of 10 MHz and 23 MHz, respectively, with $I_1 = 3 \cdot 10^{-2}$ W/cm² and $12 \cdot 10^{-2}$ W/cm². The relative amplitude of this resonance was equal to approximately 1.5–2.5 for different intensities of the orienting radiation.

The main and fundamental difference between the experimental and theoretical results is the sign of the sharp structure. According to the theory, for $\alpha = 0.34$ a dip and not a peak should be observed in the absorption spectrum of a linearly polarized probe field. This is especially true for circular polarization, used in Ref. 7. In the experiments in Ref. 7, however, a peak with a very large amplitude ($H \approx 2.5$) was observed.

On the other hand, the absolute value of the width of the observed peak (45 MHz with $I_1 = 12 \cdot 10^{-2}$ W/cm²) is of the same order of magnitude as the expected width

$$\Gamma_1 \approx \Gamma \sqrt{\kappa_1} = 70 \text{ MHz},$$

which supports the picture of Bennett dips and peaks in the velocity distribution.

The disagreement between the experimental and the theoretical results means that under the conditions of Ref. 7, besides the orienting action of the laser pump, there exists an additional mechanism for increasing the occupancy of the sublevel $n0$. This mechanism could be the anisotropy of the excitation processes, which are described by the excitation-rate matrices $Q_{MM'}$ and $q_{MM'}$, i.e., they need not be spherically symmetric.

The following interesting result of the experiments of Ref. 7 also leads to the same conclusion. For sufficiently high intensities of the orienting field ($I_1 > 0.1$ W/cm²) an even narrower dip, which becomes deeper as I_1 increases, appears at the center of the sharp absorption peak of the probe field. This dip is interpreted in Ref. 7 as being a consequence of the field-induced (Stark) splitting of the levels m and n . However, in the case of oppositely propagating waves E_1 and E_2 , the field-induced splitting, like the nonlinear interference effects, should not be observed. This dip is of a different nature, probably associated with the field-induced perturbation of the alignment, formed by anisotropic excitation (see Sec. 5). We note, finally, that in Ref. 7 the wide component of the absorption spectrum has a more complicated structure than a simple Gaussian contour. This could also be due to excitation anisotropy.

5. ABSORPTION SPECTRUM OF THE PROBE FIELD UNDER ANISOTROPIC EXCITATION

Metastable states are usually investigated under conditions of gas-discharge excitation. It is well known that the excitation in gas-discharge tubes is not isotropic; it is axisymmetric (see, for example, Refs. 4 and 5). The excitation anisotropy could be due to the anisotropy of the radiation field in the discharge tube, electron flux anisotropy, and other

factors. For our purposes here, it is not so much the reasons for the excitation anisotropy as the anisotropy itself that is important.

The form of the excitation tensor is simplest in the coordinate system in which the z' axis is directed along the axis of the tube and the x' axis is directed along the radius of the cross section of the tube.^{4,5} In this coordinate system the only nonzero components of the excitation tensor $\tilde{Q}_q^{(\kappa)}$ in the κq representation are $\tilde{Q}_0^{(0)}$, $\tilde{Q}_0^{(2)}$, and $\tilde{Q}_{\pm 2}^{(2)}$. Under a rotation of the x' axis the components with $q = \pm 2$ oscillate as $\exp(-2i\varphi)$, where φ is the azimuthal angle. For this reason, after integrating over the cross section of a light beam that is coaxial with the discharge, the components $\tilde{Q}_{\pm 2}^{(2)}$ do not contribute to the observed quantities, i.e., for what follows, only the components $\tilde{Q}_0^{(0)}$ and $\tilde{Q}_0^{(2)}$ are important.

In the transformation to a coordinate system in which the z axis is parallel to E_1 , the tensor $\tilde{Q}_q^{(\kappa)}$ is transformed by means of the Wigner \mathcal{D} matrices (see, for example, Refs. 2–5, and 9) into the tensor $Q_q^{(\kappa)}$ with the nonzero components

$$Q_0^{(0)} = \tilde{Q}_0^{(0)}, \quad Q_0^{(2)} = \frac{1}{4} \tilde{Q}_0^{(2)}, \quad Q_{\pm 2}^{(2)} = \frac{1}{4} \sqrt{\frac{3}{2}} \tilde{Q}_0^{(2)}. \quad (5.1)$$

The transformation from the κq to the JM representation, which is more convenient for our problems, is made according to the formula

$$Q_{MM'} = \sum_{\kappa q} (-1)^{J_n - M'} \langle J_n M J_n - M' | \kappa q \rangle Q_q^{(\kappa)}, \quad (5.2)$$

whence for $J_n = 2$ it follows that

$$Q_{MM} \equiv Q_M = \frac{1}{\sqrt{5}} \tilde{Q}_0^{(0)} + \frac{M^2 - 2}{\sqrt{7}} Q_0^{(2)},$$

$$Q_{20} = Q_{02} = Q_{-20} = Q_{0-2} = \frac{1}{4} \sqrt{\frac{3}{7}} \tilde{Q}_0^{(2)}, \quad (5.3)$$

$$Q_{1-1} = Q_{-11} = \frac{1}{4} \sqrt{\frac{9}{14}} \tilde{Q}_0^{(2)}.$$

The term $\tilde{Q}_0^{(0)}/\sqrt{5}$ corresponds to the isotropic part of the excitation, which appeared in Sec. 4. The terms containing $\tilde{Q}_0^{(2)}$ describe the anisotropic part of the matrix $Q_{MM'}$. It is evident from the formulas (5.3) that the axial symmetry of the excitation will cause the populations of the sublevels nM to be different and it will introduce a definite correlation between the magnetic sublevels with $|M - M'| = 2$. According to the calculations of Refs. 5 and 6, anisotropy resulting from trapping of radiation will lead to $\tilde{Q}_0^{(2)} > 0$. In this case the occupancy of the sublevels $M = 0$ and ± 1 is less than the average (over M) and the occupancy of the sublevels $M = \pm 2$ is greater than the average (we also note that Q_{1-1} is $\sqrt{3/2}$ times greater than Q_{20}).

What we have said about the anisotropy of $Q_{MM'}$ is equally true for the excitation matrix $q_{MM'}$ of the upper level.

We now consider the absorption of the probe field, taking into consideration the excitation anisotropy. The quantities ρ_{20}^j and ρ_{1-1}^j , which contribute to $\bar{\rho}_{MM'}$ (and, therefore, to P_2) satisfy the equations

$$\Gamma_m \rho_{20}^m - iG_2 \bar{\rho}_{02}^* = q_{20}; \quad (\Gamma + i\Omega_1) \bar{\rho}_{02}^* - iG_2^* \rho_{20}^m = 0; \quad (5.4)$$

$$\Gamma_n \rho_{20}^n - iG_2^* \bar{\rho}_{20} = Q_{20} + A_{1-1}^{20} \rho_{1-1}^m, \\ (\Gamma - i\Omega_1) \bar{\rho}_{20} - iG_2 \rho_{20}^n = 0, \quad (5.5)$$

$$(\Gamma - i\Omega_1) \bar{\rho}_{1-1} - iG_1 \rho_{1-1}^n - iG_{-1} \rho_{1-1}^m = 0; \\ \Gamma_n \rho_{1-1}^n - iG_1^* \bar{\rho}_{1-1} + iG_{-1} \bar{\rho}_{-11}^* = Q_{1-1}$$

$$+ \sum_{M_1 M_2} A_{M_1 M_2}^{1-1} \rho_{M_1 M_2}^m, \quad (5.6)$$

$$\Gamma_m \rho_{1-1}^m + iG_1^* \bar{\rho}_{1-1} - iG_1 \bar{\rho}_{-11}^* = q_{1-1}, \\ (\Gamma + i\Omega_1) \bar{\rho}_{-11}^* + iG_{-1}^* \rho_{1-1}^n - iG_1^* \rho_{1-1}^m = 0.$$

In Eqs. (5.4)–(5.6) the quantities $\bar{\rho}_{MM\pm 2}^*$ denote the constant amplitudes of the matrix elements:

$$\rho_{20} = \bar{\rho}_{20} \exp(-i\Omega_1 t), \quad \rho_{02}^* = \bar{\rho}_{02}^* \exp(i\Omega_1 t), \\ \rho_{1-1} = \bar{\rho}_{1-1} \exp(i\Omega_1 t), \quad \rho_{-11}^* = \bar{\rho}_{-11}^* \exp(i\Omega_1 t). \quad (5.7)$$

The terms $A_{M_1 M_2}^{MM'} \rho_{M_1 M_2}^M$ describe the radiation cascade of magnetic coherence from the upper level (m) into the lower level (n), analogous to the spontaneous particle-number cascade [see Eqs. (2.4) and (2.7)]. The rates of the coherence cascade are given by the formula²⁻⁵

$$A_{M_1 M_2}^{MM'} = A_{mn} \sum_{\sigma} \langle J_n M 1 \sigma | J_m M_1 \rangle \langle J_n M' 1 \sigma | J_m M_2 \rangle. \quad (5.8)$$

In the case $J_m = J_n = 2$ and $|M - M'| = 2$, we have

$$A_{1-1}^{20} = A_{-11}^{-20} = A_{mn} / \sqrt{6}, \quad A_{1-1}^{1-1} = -A_{mn} / 6. \quad (5.9)$$

We emphasize that the terms describing the effects which are nonlinear in the probe field are dropped on the right-hand sides of Eqs. (62)–(64).

It can be shown that under these conditions we have

$$\rho_{20}^j = \rho_{-20}^j, \quad \rho_{1-1}^j = \rho_{-11}^j = \rho_{1-1}^{j*}. \quad (5.10)$$

Taking into consideration the relations (5.10) and (4.3), we arrive at the expression (4.10) for the power P_2 absorbed from the probe field, where $N(\Omega_1)$ must be replaced by the quantity $N(\Omega_1) + N_a(\Omega_1)$, and

$$N_a(\Omega_1) = \rho_{1-1}^m - \rho_{1-1}^n + 2 \sqrt{\frac{2}{3}} \operatorname{Re}(\rho_{20}^m - \rho_{20}^n), \quad (5.11)$$

and $N(\Omega_1)$ is determined by Eq. (4.11) and determines the occupancy part of P_2 . The difference between $N(\Omega_1)$ and the expressions (4.12)–(4.15) is associated with the M dependence of the unsaturated population differences $\rho_M^0 - r_M^0$. Let

$$\rho_M^0 - r_M^0 = (\bar{\rho}^0 - \bar{r}^0)(1 + \Delta\rho_M), \quad (5.12)$$

where $\bar{\rho}^0 - \bar{r}^0$ is the M -averaged value (isotropic part) and $\Delta\rho_M$ is the relative fraction of the population difference owing to anisotropy. In agreement with Eq. (5.3), we can set

$$\Delta\rho_1 = -\frac{1}{2} \Delta\rho_2, \quad (5.13)$$

which will be approximately correct if $Q_M > q_M$. A calculation shows that when Eq. (5.13) is satisfied, the change ΔH in the amplitude H as a result of the population anisotropy is given by the formula (for $\kappa \gg 1$)

$$\Delta H = \Delta\rho_2 \frac{3}{10} \frac{1 - 23\alpha/6 + 4\alpha^2}{6 - 5\alpha}. \quad (5.14)$$

It follows from this expression that $\Delta H > 0$ holds for any α . As α decreases, the coefficient of $\Delta\rho_2$ changes from 0.35 ($\alpha = 1$) to approximately 0.01. Therefore the occupancy effect of the excitation anisotropy increases the amplitude of the sharp structure in the absorption spectrum of the probe field, if it has the form of a peak, whereas in the case of a dip it increases the depth of the dip.

We note that the occupancy effect is too small to explain the positive sign of the sharp structure of the spectrum in Ref. 7 (for $\alpha = 1/3$, we have $\Delta H \approx 0.01 \Delta\rho_2$).

The dependence of the anisotropic part $N_a(\Omega_1)$ on $\mathbf{k} \cdot \mathbf{v}$ is described by two Lorentzians with the half-widths Γ_1 and Γ_2 , and their amplitudes differ somewhat from B_1 and B_2 , i.e., the anisotropy of the occupancies in this respect does not give anything qualitatively new. In contrast to this, the properties of the correlation part of $N_a(\Omega_1)$ are much different. We find from Eqs. (5.4)–(5.6)

$$\rho_{20}^m = \frac{\Gamma + i\Omega_1}{\Gamma_5 + i\Omega_1} \frac{q_{20}}{\Gamma_m}, \quad \Gamma_5 = \Gamma \left(1 + 2 \frac{\Gamma_n}{\Gamma_m} \kappa \right), \quad (5.15)$$

$$\rho_{20}^n = \frac{\Gamma - i\Omega_1}{\Gamma_5 - i\Omega_1} \frac{1}{\Gamma_n} \left(Q_{20} + \frac{\alpha}{\sqrt{6}} \Gamma_m \rho_{1-1}^m \right), \\ \Gamma_6 = \Gamma(1 + 2\kappa), \quad (5.16)$$

$$\rho_{1-1}^m = \frac{q_{1-1}}{\Gamma_m} - \frac{\Gamma^2 \kappa}{\Gamma_7^2 + \Omega_1^2} \frac{1}{\Gamma_m} \left[Q_{1-1} + q_{1-1} \right. \\ \left. + \sqrt{\frac{2}{3}} \alpha \Gamma_m \operatorname{Re}(\rho_{02}^m) \right], \\ \Gamma_7^2 = \Gamma^2 [1 + (1 - \alpha/3)\kappa], \quad (5.17)$$

$$\rho_{1-1}^m - \rho_{1-1}^n = \frac{\alpha}{6} \frac{\Gamma_8^2 + \Omega_1^2}{\Gamma_7^2 + \Omega_1^2} \frac{1}{\Gamma_n} q_{1-1} \\ - \frac{\Gamma \Gamma_5 + \Omega_1^2}{\Gamma_7^2 + \Omega_1^2} \frac{1}{\Gamma_n} \left[Q_{1-1} \right. \\ \left. + \sqrt{\frac{2}{3}} \alpha \Gamma_m \operatorname{Re}(\rho_{20}^m) \right], \\ \Gamma_8^2 = \Gamma^2 (1 + 2\kappa \Gamma_n / A_{mn}). \quad (5.18)$$

It is evident from the relations (5.15)–(5.18) that $N_a(\Omega_1)$ can be represented as a sum of three Lorentzians

$$N_a(\Omega_1) = -C + \frac{\Gamma_5^2 C_5}{\Gamma_5^2 + \Omega_1^2} + \frac{\Gamma_6^2 C_6}{\Gamma_6^2 + \Omega_1^2} + \frac{\Gamma_7^2 C_7}{\Gamma_7^2 + \Omega_1^2}. \quad (5.19)$$

A comparatively simple expression is obtained for the coefficient C :

$$C = \frac{1}{\Gamma_n} \left(2\sqrt{2/3} Q_{20} + Q_{1-1} + \sqrt{2/3} \alpha q_{20} + \frac{\alpha}{2} q_{1-1} \right). \quad (5.20)$$

The expressions for the coefficients C_5 , C_6 and C_7 are complicated and we present them only for the most interesting case $\kappa \gg 1$, $\Gamma_m \gg \Gamma_n$:

$$C_5 = -4 \sqrt{\frac{2}{3}} \frac{\alpha^2}{1 - \alpha/3} \frac{\Gamma_n}{\Gamma_m} \kappa \frac{q_{20}}{\Gamma_m}, \quad (5.21)$$

$$C_6 = \frac{1}{\Gamma_n} \left(2 \sqrt{\frac{2}{3}} Q_{20} + \frac{2}{3} \alpha q_{1-1} \right), \quad (5.22)$$

$$C_7 = \frac{1}{\Gamma_n} \left(Q_{1-1} + \sqrt{\frac{2}{3}} \alpha q_{20} - \alpha^2 q_{1-1} \right). \quad (5.23)$$

After averaging explicitly over the velocities, the component of the absorption spectrum owing to the term $N_a(\Omega_1)$ will be described by the combination

$$\begin{aligned} & -C + C_5 \frac{\Gamma_5(\Gamma_5 + \Gamma)}{(\Gamma_5 + \Gamma)^2 + (2\Omega)^2} + C_6 \frac{\Gamma_6(\Gamma_6 + \Gamma)}{(\Gamma_6 + \Gamma)^2 + (2\Omega)^2} \\ & + C_7 \frac{\Gamma_7(\Gamma_7 + \Gamma)}{(\Gamma_7 + \Gamma)^2 + (2\Omega)^2}, \end{aligned} \quad (5.24)$$

which is essentially identical to (5.19) with $\Gamma_i \gg \Gamma$.

The correlation part of $N_a(\Omega_1)$ of the effective difference of the populations, like $N(\Omega_1)$, consists of Lorentzians, but the half-widths Γ_5 and Γ_6 are qualitatively different from the half-widths Γ_1 and Γ_2 appearing previously. For the latter widths, with $\kappa \gg 1$, characteristically we have Γ_1 , $\Gamma_2 \approx \sqrt{\kappa}$. The half-width Γ_7 also satisfies a similar law. For large κ the half-widths Γ_5 and Γ_6 have, however, a stronger dependence on the power of the orienting field:

$$\Gamma_5 \approx 2\Gamma \frac{\Gamma_n}{\Gamma_m} \kappa = 4|G_1|^2/\Gamma_m, \quad \Gamma_6 \approx 2\Gamma \kappa = 4|G_1|^2/\Gamma_n,$$

i.e., they are proportional to the intensity of the strong field and not its amplitude. In particular, under the conditions of Ref. 7 κ could reach values of the order of 10^3 , and $\Gamma_6 \approx 2\Gamma \kappa$ became comparable to the Doppler half-width ($\Gamma = 3$ MHz, $k\bar{v} = 800$ MHz).

It can be shown that the field dependence of the Γ_5 and Γ_6 relaxation rates occurs in cases when one transition is optically allowed in the three-level system and the field resonant with it "mixes" (or couples) the polarizations of the other two forbidden transitions. In our case the three-level systems are the triplets of sublevels $m0$, $m2$, $n2$ and $n0$, $n2$, $m2$. In these systems the transition $m2 - n2$ is allowed, and $m0 - m2$, $m0 - n2$ and $n0 - n2$, $n0 - m2$ are, correspondingly, optically forbidden [see Eqs. (5.4) and (5.5)]. The linear power dependence of Γ_5 and Γ_6 is also formally associated with the fact that the transition $nM - mM$ is for-

bidden for $M=0$. For this reason, such a coupling of the relaxation characteristics and κ for $|\Delta M|=2$ is possible only if $J_n = J_n \geq 2$.

We recall that the κ dependence of Γ_6 characterizes the field-induced perturbation of the M -exchange in the metastable state n . In contrast to Γ_6 , the half-width Γ_5 is associated with M -exchange in the short-lived upper level m . For this reason, the field part of the Γ_5 is proportional to κ , but it contains the small factor Γ_n/Γ_m and can differ from Γ_6 by several orders of magnitude. Specifically, under the conditions of Ref. 7, we have $\Gamma_n/\Gamma_m \sim 10^{-3}$ and $\Gamma_n \kappa/\Gamma_m \approx 1$.

The half-width Γ_7 falls between (for $\kappa \gg 1$) Γ_5 and Γ_6 :

$$\Gamma_5 \approx 2\Gamma \frac{\Gamma_n}{\Gamma_m} \kappa \ll \Gamma_7 \approx \Gamma \sqrt{\kappa} \ll \Gamma_6 \approx 2\Gamma \kappa.$$

Therefore the half-widths of the three Lorentzians comprising $N_a(\Omega_1)$ can have very different values.

The Lorentzian with the small half-width Γ_5 is "negative" ($C_5 < 0$). Therefore, according to Eqs. (5.19) and (5.24), it should be observed in the absorption spectrum as a dip which is much narrower than the rest of the structure. The amplitude C_5 becomes appreciable only for very high intensities, when $\Gamma_n \kappa/\Gamma_m \sim 1$, and it continues to increase, without saturating, as κ increases.

The above-listed properties of the Lorentzian with the half-width Γ_5 agree qualitatively with the behavior of the dip, recorded in Ref. 7 and mentioned previously in Sec. 4, at the center of the absorption line. For this reason, it can be conjectured that this observed dip appears as a result of the field-induced perturbation of the correlation between the magnetic sublevels of the upper $2p_3$ state.

The amplitudes C_6 and C_7 are positive, and the corresponding Lorentzians in the absorption spectrum should give peaks (and not dips). The sum

$$-C + C_6 + C_7 = 0 \quad (5.25)$$

($\kappa \gg 1$), i.e. for $\Omega_1 = 0$ we have $N_a = -C_5 \approx 0$ (the coefficient C_5 is small compared to the other coefficients). The equality (5.25) means that $N_a(\Omega_1)$ leads to an overall decrease of the Bennett structure in the "wings." The components C and C_6 are especially strongly manifested in this respect: C determines the velocity-nonspecific decrease of the effective population difference, similar to homogeneous broadening; C_6 is the amplitude of the Lorentzian with the large half-width, which for sufficiently large, easily achievable values of κ , can be comparable to the Doppler width.

Returning to the experimental results of Ref. 7, we can conjecture that the anomalous (positive) sign of the sharp structure of the absorption spectrum of the probe field is due to self-alignment of the neon atoms in the gas-discharge plasma, since this effect gives a positive structure. The fact that the shape of the wide component of the absorption spectrum is not Gaussian could be associated with the wide Lorentzian (C_6 , Γ_6).

6. DISCUSSION

The qualitative physical picture of the processes which make possible optical orientation of a metastable state with the aid of linearly polarized radiation is simple. The states nM , mM form a set of two-level M -subsystems in which induced transitions occur. Spontaneous cascade transitions $mM \rightarrow nM \pm 1$ cause the atoms to migrate through the M -sublevels and the two-level M -subsystems to "couple". Ultimately, the Bennett structure in the velocity distribution of the atoms turns out to be quantitatively complicated—it consists of J_m Lorentzians with different amplitudes and half-widths which depend on the intensity of the field and the branching ratio $\alpha = A_{mn}/\Gamma_n$. The half-widths are found from the roots of the characteristic polynomial of degree J_m .

In the particular case $J_m = 2$ the analysis led to the unexpected conclusion that all basic characteristics depend sensitively on α : the amplitudes of separate Lorentzians and the total Bennett structure, the half-widths Γ_1 and Γ_2 , and absorption of the orienting and probe fields (Figs. 1, 4–7). Therefore the relaxation of the upper state m through the third levels leads to a striking difference between the optical orientation of the metastable and ground states. This difference will increase with J_m , since the number of absorption and cascade re-emission events required for an atom to arrive in the state $n0$ increases and therefore the role of the relaxation through the third levels increases.

Besides the occupancy effect, described by the Bennett structure, three resonances (5.19) associated with magnetic coherence are manifested in the absorption spectrum of the probe field. Their half-widths Γ_5 , Γ_6 , and Γ_7 can differ by several orders of magnitude and the corresponding Lorentzians can form in the absorption spectrum both peaks and dips.

We underscore the fundamental novelty of the resonances (5.19) for probe-field spectroscopy. It is found that in the standard two- and three-level schemes the resonance widths for $\kappa \gg 1$ are found to be of the type $\Gamma\sqrt{\kappa}$. In our problem, however, on account of the degeneracy and anisotropy of the excitation, resonances with half-widths of the form $\Gamma\kappa$ appear.

The correlation resonances can produce not only excitation anisotropy (as shown in Sec. 5) but also effects which are nonlinear in the probe-field intensity. It can be shown, for example, that in the case of a linearly polarized field \mathbf{E}_2 orthogonal to the field \mathbf{E}_1 , the first corrections of order $|g|^4$ in P_2 are equivalent to replacing Q_{20} , Q_{1-1} , q_{20} , and q_{1-1} by

$$q_{20} + \frac{|g|^2}{\sqrt{6}} \left(\frac{\rho_0 - r_1}{\Gamma - i\Omega_2} + \frac{\rho_2 - r_1}{\Gamma + i\Omega_2} \right),$$

$$Q_{1,-1} + \frac{|g|^2\Gamma}{\Gamma^2 + \Omega_2^2} (\rho_1 - r_0),$$

$$q_{20} - \frac{|g|^2}{\sqrt{6}} \left(\frac{\rho_1 - r_0}{\Gamma + i\Omega_2} + \frac{\rho_1 - r_2}{\Gamma - i\Omega_2} \right),$$

$$q_{1,-1} - \frac{|g|^2\Gamma}{\Gamma^2 + \Omega_2^2} (\rho_0 - r_1). \quad (6.1)$$

These expressions have a more complicated dependence on v . However, the probe-field absorption spectrum will once again contain Lorentzians with the half-widths Γ_1 , Γ_2 , Γ_5 , Γ_6 , and Γ_7 , since the expression for (4.10) for P_2 contains the factor $\Gamma/(\Gamma^2 + \Omega_2^2)$, and the additional factors of a similar type that appear in the relations (6.1) do not introduce anything qualitatively new. The novelty of the expressions (6.1) appears in the new parameters on which the amplitudes of the Lorentzians will depend.

We believe that the main experimental results of Ref. 7—a peak with a width of the order of $\Gamma\sqrt{\kappa}$, a narrow dip at the center of the line, and deformation of the wide component of the line—are due to occupancy and correlation resonances.

Our analysis was based on the simplest kinetic model. This was done deliberately in order to reveal the basic characteristics of the optical orientation of metastable atoms and its manifestations. In real situations inelastic collisions with electrons and atoms, radiation trapping, transit effects, deorienting collisions, longitudinal and transverse nonuniformity of the medium and the field, an external magnetic field, and many other circumstances could be important. The richness of the manifestations of the optical orientation of metastable atoms shows that saturation-spectroscopy methods can be used to investigate these and other processes.

In conclusion, we wish to express our deep appreciation to A. M. Shalagin, A. M. Tumaikin, and I. M. Beterov for fruitful discussions and for a discussion of the results.

¹W. Happer, *Rev. Mod. Phys.* **44**, 169 (1972).

²C. G. Rautian, G. I. Smirnov, and A. M. Shalagin, *Nonlinear Resonances in Atomic and Molecular Spectra* [in Russian], Nauka, Novosibirsk, 1979.

³S. G. Rautian and A. M. Shalagin, *Kinetic Problems of Non-Linear Spectroscopy*, North-Holland, Amsterdam, 1991.

⁴M. P. Chaika, *Interference of Atomic States*, Springer, New York (1993).

⁵E. B. Aleksandrov, G. I. Khvostenko, and M. P. Chaika, *Interference of Atomic States*, Springer, New York (1993).

⁶V. S. Letokhov and V. P. Chebotayev, *Ultra-high Resolution Nonlinear Laser Spectroscopy* [in Russian], Nauka, Moscow, 1990.

⁷I. A. Kartashov and A. V. Shishaev, *Pis'ma Zh. Éksp. Teor. Fiz.* **58**, 501 (1993) [*JETP Lett.* **58**, 502 (1993)].

⁸I. I. Sobel'man, *Introduction to the Theory of Atomic Spectra*, Pergamon Press, N. Y., [Russian edition, Nauka, Moscow, 1977].

⁹D. A. Varshalovich, A. N. Moskalev, and V. K. Khersonskii, *Quantum Theory of Angular Momentum*, World Scientific, Singapore (1987).

Translated by M. E. Alferieff